Flutter and Divergence Aeroelastic Characteristics for Composite Forward Swept Cantilevered Wing

I. Lottati*
Technion—Israel Institute of Technology, Haifa, Israel

An analytical investigation was conducted to determine the aeroelastic flutter and divergence behavior of a cantilevered, composite, forward swept rectangular wing. The influence due to the variation in the bending-torsion stiffness coupling of the tailored wing on the flutter and divergence critical dynamic pressure is analyzed. The analytical approach utilizes the incompressible two-dimensional unsteady aerodynamic strip theory. Flutter and divergence velocities were obtained by using an optimization procedure that solves exactly the coupled bending-torsion equations for a cantilevered swept wing. The results indicate that the flutter and divergent of a fixed-root wing involve a compromise, since the bending-torsion stiffness that maximizes the flutter velocity tends to minimize the divergent speed and vice versa.

Introduction

AEROELASTIC tailoring is broadly defined as the technology to design a lifting surface that exhibits a desired aeroelastic response. The desired aeroelastic responses most often considered are the maximization of flutter and divergence speeds, although others can also be important.

Aeroelastic tailoring of a lifting surface involves the synthesis of a composite structure whose special directional properties elastically couple the basic structural deformations, such as bending and torsion, in an advantageous manner. The purpose of this paper is to investigate the critical flutter and divergence velocities of a swept wing as influenced by the bending-torsion stiffness coupling of a composite cantilevered wing.

Aeroelastic tailoring, which exploits the anisotropic character of advanced composites, has received considerable attention in the literature due to the renewed interest in forward swept wing technology. Krone[1] concluded that forward swept wings without divergence or weight penalties may be possible through the use of selectively laminated advanced composites. Weisshaar[2,3] analytically extended Krone's conclusions to potentially practical wing designs. Weisshaar concluded that the bending-torsion stiffness coupling of anisotropic advanced composite materials could be used to alleviate divergence in forward swept wings. Sherrer et al.[4] conducted a series of wind tunnel tests using simple plate-like models of a forward swept wing. These tests essentially verified Weisshaar's conclusion and also showed that existing analytical techniques such as computer programs could adequately predict the divergence dynamic pressures for most test conditions. Still, there is only a very limited amount of wind tunnel data available that examines the effect of structural bending-torsion coupling on flutter speed or that verifies the accuracy of analytical predictions. An investigation to determine the effect of bending-torsion stiffness coupling on both the divergence and flutter velocities of unswept cantilevered wings was conducted by Hollowell and Dugundji.[5]

Received Jan. 16, 1985; revision received June 24, 1985.

*Senior Lecturer, Department of Aeronautical Engineering.

Analytical Model

This analysis considers a high-aspect-ratio forward swept wing, idealized by a box beam whose planform is shown in Fig. 1a, that derives all of its bending-torsion stiffness coupling from the laminated composite upper and lower skins (stiffness from spars, ribs, webs could be added algebrically to those of the plate) and is subjected to airflow V. The fiber orientation relative to the spanwise reference axis is shown in Fig. 1b. The displacement assumptions are shown in Fig. 1c.

It is assumed that the resulting box beam wing structure is such that its deformation may be represented by a bending deflection $h(y)$, positive downward, along a straight reference axis (the rotation axis in Fig. 1a) and a rotation $\alpha(y)$, positive nose up, about this axis. In addition, it is further assumed that the wing chordwise sections, perpendicular to the beam's reference axis, are rigid so that the wing deformation is a function only of the spanwise coordinate y. Hence, the deformation is assumed of the form

$$w(x,y) = h(y) + x_a \alpha(y) \tag{1}$$

where $x_a = x - ba$. An identical structure model was used by Weisshaar[3] and Oyibo[6] to study the divergence of swept laminated composite wings.

Using the box beam model, equivalent bending and torsional stiffness of the wing, EI_b and GJ, respectively, may be computed employing the strain energy method. The strain energy U for a symmetric anisotropic laminate plate is given as[7]

$$U = \frac{1}{2}\int_0^1 \int_{-b}^{b} \left[D_{11}\left(\frac{\partial^2 w}{\partial x^2}\right)^2 + 2D_{12}\frac{\partial^2 w}{\partial x^2}\frac{\partial^2 w}{\partial y^2} + D_{22}\left(\frac{\partial^2 w}{\partial y^2}\right)^2 + 4D_{16}\frac{\partial^2 w}{\partial x^2}\frac{\partial^2 w}{\partial x \partial y} + 4D_{26}\frac{\partial^2 w}{\partial y^2}\frac{\partial^2 w}{\partial x \partial y} + 4D_{66}\left(\frac{\partial^2 w}{\partial x \partial y}\right)^2 \right] dx\,dy \tag{2}$$

where D_{ij} are the flexural moduli for an N-ply laminate with ply angle orientation θ (see Fig. 1b) and w the transverse deflection of the plate, positive downward.

The kinetic energy is given by

$$T = \frac{1}{2}\int_0^1 \int_{-b}^{b} \left(\frac{\partial w}{\partial t}\right)^2 \rho(x,y)\,dx\,dy \tag{3}$$

where $\rho(x,y)$ is the material density of the wing.

The virtual work expression is given by

$$\delta W = \int_0^1 (-L\delta w + M\delta\alpha)\mathrm{d}y \tag{4}$$

where L is the aerodynamic lift, positive upward, and M the aerodynamic moment about the wings elastic axis, positive nose up.

Applying the principle of minimum potential energy, one gets the following governing differential equations:

$$EI_b\frac{\partial^4 h}{\partial y^4} + d_{22}\frac{\partial^4\alpha}{\partial y^4} + K\frac{\partial^3\alpha}{\partial y^3} + m\frac{\partial^2 h}{\partial t^2} + mX_\alpha\frac{\partial^2\alpha}{\partial t^2} = -L$$

$$d_{22}\frac{\partial^4 h}{\partial y^4} - K\frac{\partial^3 h}{\partial y^3} + S\frac{\partial^4\alpha}{\partial y^4} - GJ\frac{\partial^2\alpha}{\partial y^2} + mX_\alpha\frac{\partial^4 h}{\partial t^2} + I_\alpha\frac{\partial^2\alpha}{\partial t^2} = M \tag{5}$$

where

$EI_b\left(=\int_{-b}^{b} D_{22}\mathrm{d}x\right)$ = beam bending stiffness

$GJ\left(=4\int_{-b}^{b} D_{66}\mathrm{d}x\right)$ = torsional stiffness

$K\left(=2\int_{-b}^{b} D_{26}\mathrm{d}x\right)$ = bending-torsion coupling stiffness

$S\left(=\int_{-b}^{b} D_{22}x_a^2\mathrm{d}x\right)$ = torsional stiffness due to rigidity in tension (warping effect)

$m\left(=\int_{-b}^{b}\rho\mathrm{d}x\right)$ = mass per unit span

$X_\alpha\left(=\frac{1}{m}\int_{-b}^{b}\rho x_a\mathrm{d}x\right)$ = center of mass offset from its elastic axis (positive aft)

$I_\alpha\left(=\int_{-b}^{b}\rho x_a^2\mathrm{d}x\right)$ = section mass moment of inertia (per unit span) about its elastic axis

$d_{22}\left(=\int_{-b}^{b} D_{22}x_a\mathrm{d}x = -abEI_b\right)$ = coupling terms due to $a\neq 0$

$d_{26}\left(=2\int_{-b}^{b} D_{26}x_a\mathrm{d}x = -abK\right)$

The boundary conditions are, for $y=0$ (root section)

$$h = \frac{\mathrm{d}h}{\mathrm{d}y} = \alpha = \frac{\mathrm{d}\alpha}{\mathrm{d}y} = 0 \tag{6a}$$

for $y=l$ (l stands for the wing semispan)

$$EI_b\frac{\mathrm{d}^3 h}{\mathrm{d}y^3} + d_{22}\frac{\mathrm{d}^3\alpha}{\mathrm{d}y^3} + K\frac{\mathrm{d}^2\alpha}{\mathrm{d}y^2} = 0$$

$$EI_b\frac{\mathrm{d}^2 h}{\mathrm{d}y^2} + d_{22}\frac{\mathrm{d}^2\alpha}{\mathrm{d}y^2} + K\frac{\mathrm{d}\alpha}{\mathrm{d}y} = 0$$

$$-d_{22}\frac{\mathrm{d}^3 h}{\mathrm{d}y^3} + K\frac{\mathrm{d}^2 h}{\mathrm{d}y^2} - S\frac{\mathrm{d}^3\alpha}{\mathrm{d}y^3} + GJ\frac{\mathrm{d}\alpha}{\mathrm{d}y} = 0$$

$$d_{22}\frac{\mathrm{d}^2 h}{\mathrm{d}y^2} + S\frac{\mathrm{d}^2\alpha}{\mathrm{d}y^2} + d_{26}\frac{\mathrm{d}\alpha}{\mathrm{d}y} = 0 \tag{6b}$$

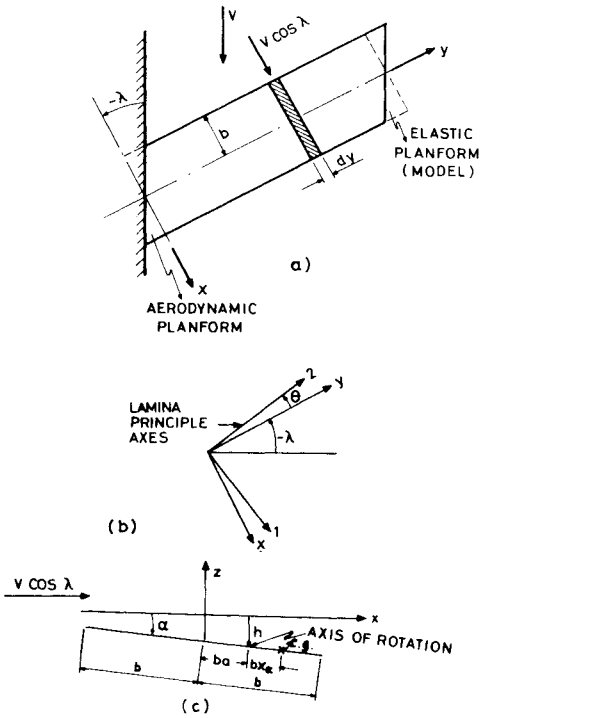

Fig. 1 Slender swept wing planform, lamina orientation, and displacement assumptions.

It should be noted that the Oyibo[6] formulation is almost identical to the present expressions if one neglects the coupling terms d_{22} and d_{26}. Furthermore, for zero warping, $S=0$, the present formulation is identical to the usual bending-torsion formulation.[8]

The aerodynamics required to solve these aeroelastic equations generally varies in levels of sophistication. Due to the complexity of the problem and in order to establish trends, simple aerodynamics shall be employed using strip theory formulation. The unsteady aerodynamic expressions for the lift and moment are developed in Ref. 8. There are some weaknesses in the velocity component strip theory for swept wings (as mentioned by Ref. 8) due to the way the vortex sheets are actually shed from the swept wings and the way they are simulated in the theory. However, for lack of a more accurate aerodynamic strip theory, the expressions of Ref. 8 are introduced in the calculations, noting that the inaccuracy increases as the sweep angles of the wing increases.

The expressions for the aerodynamic forces are as follows:

$$L(y,t) = \pi\rho b\left\{b\left(\frac{\partial^2 h}{\partial t^2} + V\frac{\partial\alpha}{\partial t}\cos\lambda + V\frac{\partial^2 h}{\partial t\partial y}\sin\lambda - ba\frac{\partial^2\alpha}{\partial t^2} - baV\frac{\partial^2\alpha}{\partial t\partial y}\sin\lambda\right) + 2V\cos\lambda C(k)\left[\frac{\partial h}{\partial t} + V\alpha\cos\lambda + V\frac{\partial h}{\partial y}\sin\lambda + ba_1\left(\frac{\partial\alpha}{\partial t} + V\frac{\partial\alpha}{\partial y}\sin\lambda\right)\right]\right\}$$

$$M(y,t) = \pi\rho b^2\left\{-b\left[Va_1\frac{\partial\alpha}{\partial t}\cos\lambda + \frac{1}{2}V^2\frac{\partial\alpha}{\partial y}\cos\lambda\sin\lambda - a\frac{\partial^2 h}{\partial t^2} - Va\frac{\partial^2 h}{\partial t\partial y}\sin\lambda + ba_3\left(\frac{\partial^2\alpha}{\partial t^2} + V\frac{\partial^2\alpha}{\partial t\partial y}\sin\lambda\right)\right] + 2V\cos\lambda C(k)a_2\left[\frac{\partial h}{\partial t} + V\alpha\cos\lambda + V\frac{\partial h}{\partial y}\sin\lambda + ba_1\left(\frac{\partial\alpha}{\partial t} + V\frac{\partial\alpha}{\partial y}\sin\lambda\right)\right]\right\} \tag{7}$$

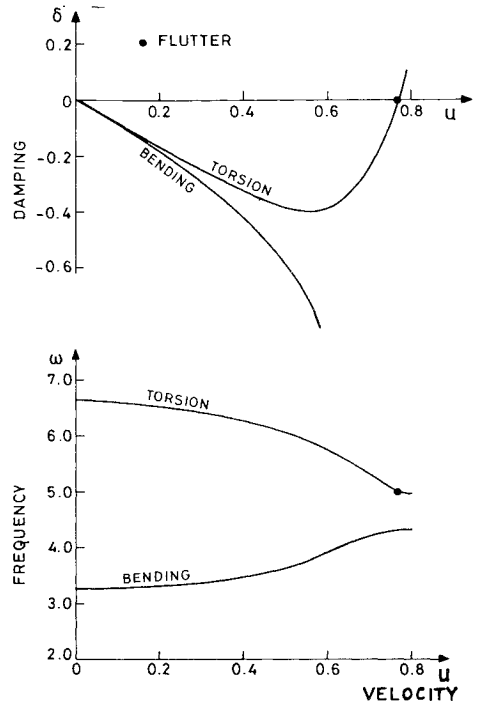

Fig. 2 Frequency and damping of the fundamental aeroelastic modes vs dimensionless air speed.

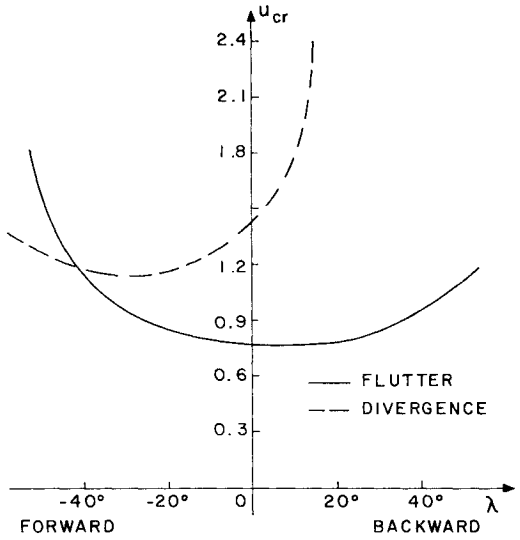

Fig. 3 Flutter and divergence velocities of a typical metallic wing with changes in sweep angle of the wing.

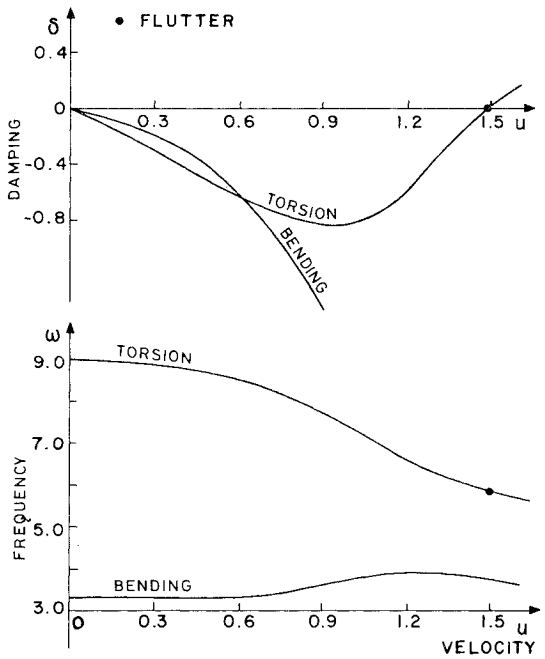

Fig. 4 Frequency and damping of the fundamental aeroelastic modes vs air speed while including the d_{22}, d_{26}, and S terms.

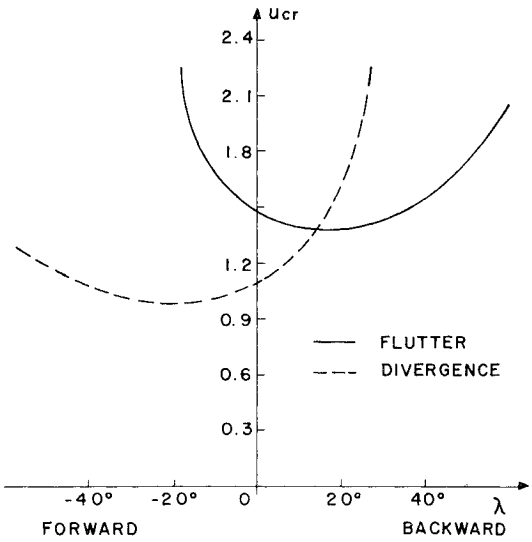

Fig. 5 Flutter and divergence velocities of a typical metallic wing with changes in sweep angle of the wing while including the d_{22}, d_{26}, and S terms.

where λ is the sweep angle of the wing (positive backward), $C(k)$ the Theodorsen circulation function, $k(=b\bar{\omega}/V\cos\lambda)$ the reduced frequency of oscillation, and $a_1=\frac{1}{2}-a$, $a_2=\frac{1}{2}+a$, $a_3=\frac{1}{8}+a^2$. To simplify calculation of the Theodorsen function $C(k)$, the approximation of Ref. 9 was used, namely

$$C(k)=\frac{0.021573+0.210400k+0.512607k^2+0.500502k^3}{0.021508+0.251239k+1.035378k^2+k^3}$$

$$-i\frac{0.001995+0.327214k+0.122397k^2+0.000146k^3}{0.089318+0.934530k+2.481481k^2+k^3} \quad (8)$$

where $i=\sqrt{-1}$.

Assuming an exact solution of the forms

$$h/b=He^{r\eta}e^{\sigma\tau} \quad \text{and} \quad \alpha=Ae^{r\eta}e^{\sigma\tau} \quad (9)$$

where $\eta=y/l$ and $\tau=\sqrt{EI_b/ml^4}\,t$ are the nondimensional spanwise coordinate and time and $\sigma=\delta+i\omega$, where δ is the damping and ω the frequency of the oscillating wing (assumed real).

Incorporating the expressions for the assumed solution [Eq. (9)] in governing equations (5) and the boundary conditions (6), one gets the following nondimensional set of equations:

$$(r^4+\sigma^2+QL_h)H+(-ar^4+k_\alpha r^3+x_\alpha\sigma^2+QL_\alpha)A=0$$

$$(-ar^4-k_\alpha r^3+x_\alpha\sigma^2-QM_h)H$$

$$+(s_\alpha r^4-g_\theta r^2+I_\theta\sigma^2-QM_\alpha)A=0 \quad (10)$$

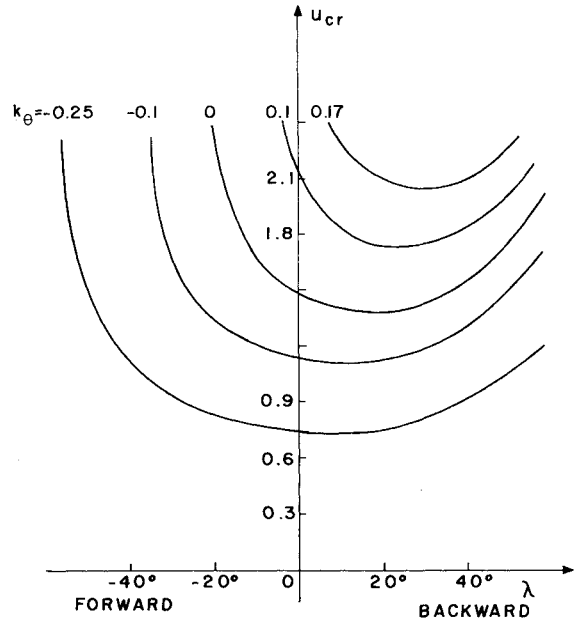

Fig. 6 Variation of flutter velocity vs sweep angle for various values of coupled bending-torsion stiffness k_θ.

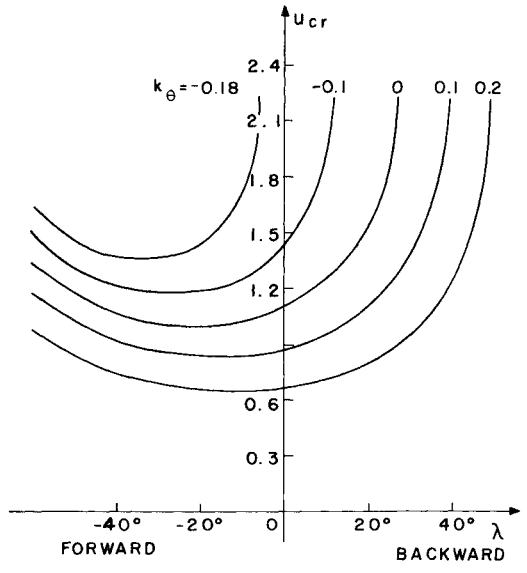

Fig. 7 Variation of divergence speed vs sweep angle for various values of coupled bending-torsion stiffness k_θ.

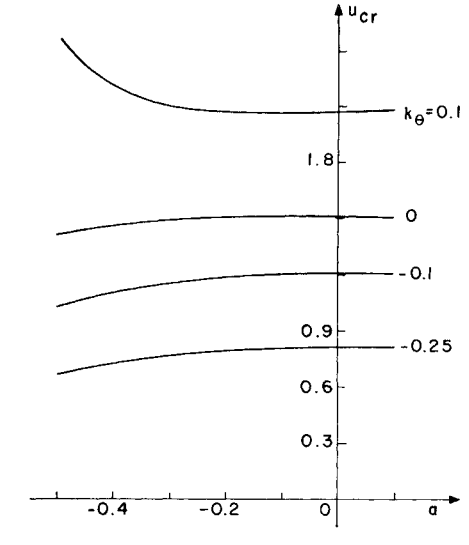

Fig. 8 Variation of flutter velocity vs position of the reference axis of rotation for various values of coupled bending-torsion stiffness k_θ.

where

$$x_\alpha = X_\alpha/b, \quad AR = l/b, \quad k_\theta = K/EI_b$$

$$k_\alpha = k_\theta AR, \quad s_\alpha = S/b^2EI_b, \quad g_g = GJ/EI_b$$

$$g_\theta = (AR)^2 g_g, \quad I_\theta = I_\alpha/mb^2, \quad Q = \pi\rho V^2 l^4/EI_b$$

$$L_h = [k_k^2 + 2\cos\lambda C(k)k_k] + (\sin\lambda/AR)[k_k + 2\cos\lambda C(k)]r$$

$$L_\alpha = [k_k\cos\lambda - ak_k^2 + 2\cos\lambda C(k)(\cos\lambda + a_1 k_k)]$$
$$+ (\sin\lambda/AR)[-ak_k + 2\cos\lambda C(k)a_1]r$$

$$M_h = [ak_k^2 + 2\cos\lambda C(k)a_2 k_k]$$
$$+ (\sin\lambda/AR)[ak_k + 2\cos\lambda C(k)a_2]r$$

$$M_\alpha = [-a_1 k_k\cos\lambda - a_3 k_k^2 + 2\cos\lambda C(k)a_2(\cos\lambda + a_1 k_k)]$$
$$+ (\sin\lambda/AR)[-\tfrac{1}{2}\cos\lambda - a_3 k_k + 2\cos\lambda C(k)a_1 a_2]r \qquad (11)$$

where $k_k = \bar{\omega}b/V[\bar{\omega} = \sqrt{EI_b/ml^4}\,\omega]$.

The boundary conditions are:
for $\eta = 0$ (root section)

$$H = rH = A = rA = 0 \qquad (12a)$$

and for $\eta = 1$ (tip section)

$$[r^3H + (-ar^3 + k_\alpha r^2)A]e^r = 0$$

$$[r^2H + (-ar^2 + k_\alpha r)A]e^r = 0$$

$$[(ar^3 + k_\alpha r^2)H + (-s_\alpha r^3 + g_\alpha r)A]e^r = 0$$

$$[-ar^2H + (s_\alpha r^2 - ak_\alpha r)A]e^r = 0 \qquad (12b)$$

To obtain a nontrivial solution, the determinant of the system of equations (10) has to be zero. Thus,

$$\Delta(r,\sigma) = \begin{vmatrix} r^4 + \sigma^2 + QL_h & -ar^4 + k_\alpha r^3 + x_\alpha\sigma^2 + QL_\alpha \\ -ar^4 - k_\alpha r^3 + x_\alpha\sigma^2 - QM_h & s_\alpha r^4 - g_\theta r^2 + I_\theta\sigma^2 - QM_\alpha \end{vmatrix} = 0 \qquad (13)$$

For prescribed σ, the characteristic equation (13) has to be solved to obtain the roots r_i. Knowing r_i, the boundary conditions in Eq. (12) that supply a system of eight linear equations have to be fulfilled. The determinant of this system of equations has to be equal to zero $[\Delta_b(r,\sigma) = 0]$ to satisfy the boundary conditions of the problem.

The combination of ω and Q (minimum) fulfilling the conditions $\Delta(r,\sigma) = 0$ and $\Delta_b(r,\sigma) = 0$ that will bring the system from neutral stability ($\delta = 0$) to instability ($\delta > 0$) are the conditions at which the wing will undergo dynamic ($\omega \neq 0$) or static ($\omega = 0$) instability.

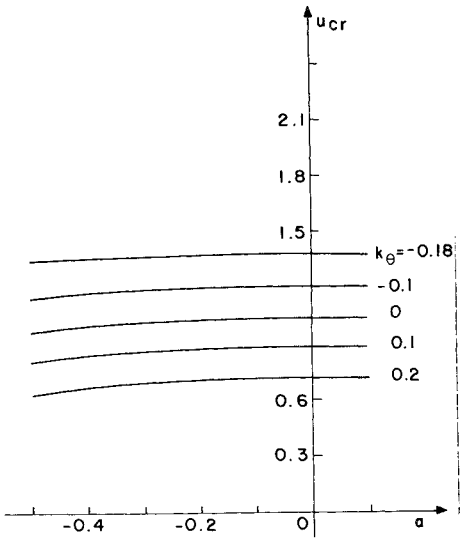

Fig. 9 Variation of divergence speed vs the position of the reference axis of rotation for various values of coupled bending-torsion stiffness k_θ for a forward swept wing ($\lambda = -30$ deg).

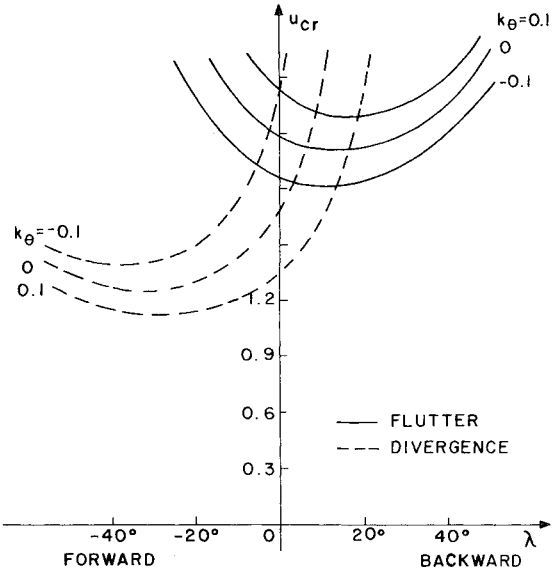

Fig. 10 Flutter and divergence velocities of a typical composite wing with change in sweep angle for various values of coupled bending-torsion stiffness k_θ.

Applications

The numerical procedure of solution is outlined in the Appendix. As stated, the process of the solution has to start from a known quantity. For the flutter problem, one has to deal with an unswept wing ($\lambda = 0$) assuming $k_\alpha = s_\alpha = x_\alpha = Q = d_{22} = d_{26} = 0$. For the assumption $\rho = 0$, the problem is reduced to an uncoupled bending-torsion cantilevered oscillating beam. For the case $\rho \neq 0$, one gets

$$\frac{\partial^4 H}{\partial \eta^4} + \frac{\partial^2 H}{\partial \tau^2} = \frac{\pi \rho b^2}{m}\left(-\frac{\partial^2 H}{\partial \tau^2} + a\frac{\partial^2 \alpha}{\partial \tau^2}\right)$$

$$-g_\theta \frac{\partial^2 \alpha}{\partial \eta^2} + I_\theta \frac{\partial^2 \alpha}{\partial \tau^2} = \frac{\pi \rho b^2}{m}\left(a\frac{\partial^2 H}{\partial \tau^2} - a_3\frac{\partial^2 \alpha}{\partial \tau^2}\right) \quad (14)$$

For the case $\rho = 0$, the first bending mode's frequency is $\omega_h = 3.52$ and the frequency of the first torsion mode is $\omega_\alpha = (\pi/2)\sqrt{g_\theta / I_\theta}$ (while $\delta = 0$). Starting from those known frequencies, one can trace the variation in ω_h and ω_α while varying ρ to the desired value. At this state, one can freeze the value of ρ and start varying x_α to the desired value. For this configuration of ρ and x_α, we can increase the flow velocity on the wing while tracing the variation in the frequencies and damping of the oscillating wing. For illustrative purposes, the method is applied on Goland's[10] typical wing with the following properties:

$m = 0.746$ slug/ft $\quad I_\alpha = 1.943$ slug·ft^2/ft

$x_\alpha = 0.1997$ $\quad EI_b = 23.6 \times 10^6$ lb·ft^2

$GJ = 2.39 \times 10^6$ lb·ft^2 $\quad \rho = 2.3769 \times 10^{-3}$ slug/ft^3

$b = 3$ ft $\quad l = 20$ ft $\quad a = -0.34$

To test the efficiency and accuracy of the present numerical method and for the sake of comparison, the classical bending torsion formulation[8] is considered first (hence $d_{22} = d_{26} = S = 0$).

Figure 2 presents the variation of the frequencies and damping of the first bending and torsion modes vs the nondimensional velocity of the flow ($u = V/V_{\text{ref}}$ where $V_{\text{ref}} = 400$ mph). Figure 2 illustrates how the frequency of the bending mode increases while the frequency of the torsion mode decreases as a function of the increasing velocity u. The flutter instability occurs while the damping of the torsion mode changes sign (from negative to positive through $\delta = 0$). It should be recalled that the results displayed in Fig. 2 are accurate at the flutter condition ($\delta = 0$) only, due to the fact that the air forces have not been introduced in a sufficiently general form to account for possible covergent or divergent oscillations. It should be noted that the air forces as derived by Theodorsen[11] are restricted to the condition when the wing moves through the air at the flutter speed, so that disturbance causes the wing to oscillate sinusoidally and at constant amplitude. Nevertheless, the frequency and damping of the fundamental aeroelastic modes plotted in Fig. 2 have the same trend as the results obtained by Goland and Luke[12] who determined the lift and moment in an approximate fashion from the indicial functions for the incompressible flow. The solution obtained by the present method ($u_{cr} = 0.766$ and $\omega = 4.974$) is identical to the corrected results reported in Refs. 13 and 14. Tracing higher modes for instability reveals that the second bending mode experienced flutter at $u = 2.53$ and $\omega = 22.83$, a very high critical velocity compared to the first torsion flutter speed.

Starting from the known solution of the flutter for the unswept wing, one can trace the variation of the flutter velocity due to variation of the sweep angle of the wing. Figure 3 shows the flutter speed behavior of this metallic wing as it is swept fore and aft. For flutter, forward sweep proves to be slightly more stabilizing than aft sweep due to the favorable aerodynamic coupling in the forward sweep configuration.

There is an analytical exact solution to compute the divergence velocity for an unswept wing. For an unswept wing, the divergence dynamic pressure is given as $Q_D = \pi^2 g_\theta / 8a_2$ ($e = a_2$ is the distance between the elastic axis and aerodynamic center). Knowing the divergence velocity for the unswept wing, one can apply the optimization procedure to trace the variation of the divergence velocity while varying the angle of sweep of the wing. It should be noted that the optimization code deals with only one parameter while computing the divergence velocity. Figure 3 shows the variation of the divergence velocity vs the sweep angle of the wing. The variation of the divergence speed, displayed in Fig. 3, is in excellent agreement with the expression given by Weisshaar.[15] Diedrich and Budiansky[16] obtained a solution for the case of slender tapered wings in which the chord is assumed to vary linearly and the bending and torsional stiffness are assumed to vary as the fourth power of the chord. In this solution, the swept forward wing is accompanied by a rapid decrease in the

divergence velocity of the wing (due to the large value of $g_g = 1$ compared to $g_g = 0.101$ in the present example). It should be noted that beyond a certain swept forward angle, the divergence speed tends to increase due to the fact that the effective velocity on the wing is reduced by the factor of $\cos\lambda$. Figure 3 shows a moderate decrease in the divergence velocity for a forward sweep angle reaching minimum around $\lambda \simeq -30$ deg and then a moderate increase in the divergence velocity as the sweep forward angle increases ($\lambda < -30$ deg). The results of Fig. 3 are not typical. In most cases, divergence is the critical mode of instability of a forward swept wing. This finding is due to the fact that, while rotating the laminate in order to obtain the coupled bending-torsion stiffness, the g_g parameter is increased appreciably.[4] The influence of increasing g_g on flutter and divergence will be addressed later in this section.

As can be seen from the characteristic equation (13), the coupling terms d_{22} and d_{26} and the parameter S can significantly affect the stability behavior of the system. The inclusion of these parameters increases the degree of the characteristic equation from the sixth to the eight power. Furthermore, these parameters affect the boundary conditions of the problem and thus potentially might influence the results. Figure 4 presents the variation of the frequencies and damping of the first bending and torsion modes vs the velocity u taking into account the coupling terms d_{22}, d_{26}, and $s_\alpha = \frac{1}{3} + a^2$. The main effect of including the d_{22}, d_{26}, and S terms results in the increasing of the frequency of the torsion mode (due to the warping effect). It should be emphasized that the flutter velocity obtained while including the d_{22}, d_{26}, and S terms is almost twice Goland's basic flutter solution ($u_{cr} = 1.481$ compared to $u_{cr} = 0.766$). Thus, the wing is gaining rigidity in the torsion mode due to the warping effect.[17] The results reported in Ref. 17 indicate that the influence of the warping effect is to increase the divergence speed due to the increase in the rigidity in the torsion mode. Figure 5 shows the variation of the flutter velocity and the divergence speed vs the sweep angle of the wing taking into account the coupling terms d_{22}, d_{26}, and S. The comparison of the results of Figs. 3 and 5 reveals that the divergence speed of the system, while including d_{22}, d_{26}, and S, is significantly lower than the divergence speed obtained without those terms. This fact indicates that the divergence speed is strongly influenced by the coupling terms d_{22} and d_{26}, which are functions of the parameter a (the location of the reference axis). It should be mentioned that the d_{22} and d_{26} influenced the divergence speed through the characteristic equations and the boundary conditions of the system. The results reported hereafter in this paper are computed while including the d_{22}, d_{26}, and S terms due to their major influence on the stability behavior of the system.

Next, the influence of the bending-torsion stiffness coupling on the flutter and divergence velocity is investigated. The bending-torsion stiffness coupling k_θ is a function of the fiber orientation angle θ of the lamina and the number N of the composite material layers forming the cover sheet of the wing.[4,7] The variation of the flutter velocity vs sweep angle for various values of the bending-torsion stiffness coupling k_θ are plotted in Fig. 6. The variation of the divergence speed vs sweep angle for various values of k_θ are plotted in Fig. 7. A positive coupling k_θ increases the flutter velocity while decreasing the divergence speed of the wing compared to an isotropic material (a zero stiffness coupling). A negative coupling k_θ decreases the flutter velocity while increasing the divergence velocity of the wing compared to an isotropic material. The results plotted in Figs. 6 and 7 indicate that passive stability enhancement by aeroelastic tailoring of the k_θ parameter involves a compromise, since maximizing divergence speed tends to minimize flutter velocity and vice versa. A similar trend of influence of the cross-coupling stiffness was reported recently by Weisshaar and Ryan.[18]

From the numerous parameters affecting the flutter and divergence of the above wing, we have chosen to investigate the influence of the variation of the position of the reference axis of rotation (the a parameter) on the stability behavior of the wing.

Figure 8 shows the flutter velocity of the system vs parameter a. The results of Fig. 8 do not show the usual trend, namely, the flutter speed does not decrease as the reference axis of the rotation moved aft (increasing the distance between the wing's axis of rotation and the aerodynamic center $e = \frac{1}{2} + a$). The results of Fig. 8 show different trends for the positive and negative values of k_θ. The variation of the divergence speed vs parameter a for different values of k_θ is shown in Fig. 8 for a forward swept wing ($\lambda = -30$ deg). The results of Fig. 9 indicate that the divergence speed remains almost constant while parameter a is varied. The results of Figs. 8 and 9 indicate the strong influence that the d_{22} and d_{26} (function of a) have on the flutter velocity and the divergence speed through the characteristic equation and the boundary conditions of the system.

To get a typical example of a composite forward swept wing, parameter g_g was almost tripled to $g_g = 0.301$. Figure 10 shows the variation of the flutter and divergence velocity (for $g_g = 0.301$) vs the sweep angle for various values of the coupled bending-torsion stiffness. The results shown in Fig. 10 support the previous findings of Figs. 6 and 7 that the coupled bending-torsion stiffness affects the flutter velocity in an opposite trend to that of the divergence speed.

It should be noted that it is relatively more difficult to select a representative wing for flutter than for static aeroelastic studies, since inertia properties enter into the analysis. Thus, even though these aeroelastic studies should not be used to form general conclusions, it is interesting to note that the coupled bending-torsion stiffness indicate the same trend of influence for the limited parametric studies represented in this paper.

Conclusions

A unified presentation of the computed flutter and divergence velocity is essential due to the fact that variation of the investigated parameter can influence the flutter velocity and divergence speed of the swept wing differently. An important conclusion predicted by this investigation is that passive stability enhancement involves a compromise on the value of the bending-torsion stiffness coupling. An attempt to eliminate the divergence of a swept forward wing by the composite bending-torsion stiffness coupling might appreciably and undesirably lower the flutter velocity of the wing.

It is shown that the warping effect and the coupling terms d_{22} and d_{26} have a strong influence on the static and dynamic behavior of the system. These terms should be included in the analysis whenever the stability behavior of the system is investigated.

The suggested optimization procedure was found to be very efficient and accurate in tracing the instability regions of the wing.

Appendix

The solution procedure begins by assuming values for ω and Q (while $\delta = 0$) and solving Eq. (13) for the roots r_i and keeps changing the combination ω and Q to meet the condition of zero determinant of the boundary condition system. To obtain a solution of the above, a solution procedure was developed that takes advantage of an optimization code that changed parameters ω and Q until a minimum is reached for the absolute value of the determinant $\Delta_b(r,\sigma)$. The difficulty in this procedure is that the determinant is a multiminimum valued function (for a different combination of ω, Q); thus, the coverged solution will be a function of the initial conditions selected for ω, Q. Usually, if the initial conditions are not close to the actual neutral stability condition, the optimization procedure will converge to the trivial solution $\omega = Q = 0$. To overcome these difficulties, one has to start the process from a known (nontrivial) solution of a simple case of the problem

and proceed by changing slowly those parameters of the system whose effect is of interest until the desired combination of parameters of the system is reached. At each step, the optimization code gets as initial conditions the converged solution of the preceding step. If one parameter is changed at a time by a small increment, it is possible to obtain a converged solution for any combination of parameters needed. The suggested solution procedure is very convenient due to the fact that the optimization code deals with only two parameters and thus the converged solution is reached within very few iterations. The calculations were done using the IBM double-precision mode to get accurate results.

It should be noted that the suggested procedure for computing the critical velocity of instability is based on the assumption that using the previous lowest flutter speed as an initial guess is reasonable so long as the lowest flutter speed or its associated frequency does not change discontinuously as the parameter is incrementally increased. However, it may happen that as the parameter is increased, a lower flutter speed may appear whose associated mode shape is different from that at the previous parameter value. This situation implies that the lowest flutter speed or its associated frequency have changed discontinuously with the parameter increment. Tracing higher modes of instability may avoid overlooking modes of lower critical flutter speed while the parameter is increased.

References

[1]Krone, N. J., "Divergence Elimination with Advanced Composites," AIAA Paper 75-1009, 1975.

[2]Weisshaar, T. A., "The Influence of Aeroelasticity on Swept Composite Wings," AFWAL-TR-80-3137, Nov. 1980.

[3]Weisshaar, T. A., "Aeroelastic Tailoring of Forward Swept Composite Wings," *Journal of Aircraft*, Vol. 18, Aug. 1981, pp. 669-676.

[4]Sherrer, V. C., Hertz, T. J., and Shirk, M. H., "Wind Tunnel Demonstration of Aeroelastic, Tailoring Applied to Forward Swept Wings," *Journal of Aircraft,* Vol. 18, Nov. 1981, pp. 976-983.

[5]Hollowell, S. J. and Dugundji, J., "Aeroelastic Flutter and Divergence of Stiffness Coupled, Graphite/Epoxy Cantilevered Plates," *Journal of Aircraft*, Vol. 21, Jan. 1984, pp. 69-76.

[6]Oyibo, G. A., "Generic Approach to Determine Optimum Aeroelastic Characteristics for Composite Forward-Swept-Wing Aircraft," *AIAA Journal,* Vol. 22, Jan. 1984, pp. 117-123.

[7]Ashton, J. E. and Whitney, J. M., *Theory of Laminated Plates*, Technonic Publishing Co., Stamford, CT, 1970.

[8]Bisplinghoff, R. L., Ashley, H., and Halfman, R. L., *Aeroelasticity,* Addison-Wesley Publishing Co., Reading, MA, 1955, Chap. 7.

[9]*Manual on Aeroelasticity,* Vol. 6, edited by W. P. Jones, NATO.

[10]Goland, M., "The Flutter of a Uniform Cantilever Wing," *Journal of Applied Mechanics*, Vol. 12, No. 4, Dec. 1945, pp. A197-A208.

[11]Theodorsen, T., "General Theory of Aerodynamic Instability and the Mechanism of Flutter," NACA TR 496, 1934.

[12]Goland, M. and Luke, Y. L., "A Study of the Bending-Torsion Aeroelastic Modes for Airplane Wings," *Journal of the Aeronautical Sciences*, Vol. 16, July 1949, pp. 389-396.

[13]Housner, J. M. and Stein, M., "Flutter Analysis of Swept-Wing Subsonic Aircraft with Parameter Study of Composite Wings," NASA TN D-7539, Sept. 1974.

[14]Goland, M. and Luke, Y. L., "The Flutter of a Uniform Wing with Tip Weights," *Journal of Applied Mechanics*, Vol. 15, No. 1, March 1948, pp. 13-20.

[15]Weisshaar, T. A. "Aeroelastic Stability and Performance Characteristics of Aircraft with Advanced Composite Swept Forward Wing Structures," AFFDL-TR-78-116, Sept. 1978.

[16]Diederich, F. W. and Budiansky, B., "Divergence of Swept Wings," NACA TN 1680, Aug. 1948.

[17]Petre, A., Stanescu, C., and Librescu, L., "Aeroelastic Divergence of Multicell Wings Taking Their Fixing Restraints into Account," *Revue de Mechanique Appliquee,* Vol. 12, No. 6, 1961, pp. 689-698.

[18]Weisshaar, T. A. and Ryan, R. J., "Control of Aeroelastic Instabilities Through Elastic Cross-Coupling," AIAA Paper 84-0906, May 1984.